Magazine of Civil Engineering

ISSN 2712-8172

journal homepage: http://engstroy.spbstu.ru/

DOI: 10.18720/MCE.99.7

Transition factor between elastic and deformation moduli for dispersive soils

V.V. Antipov*, V.G. Ofrikhter
Perm National Research Polytechnic University, Perm, Russia
** E-mail: seekerva@mail.ru*

Keywords: Multichannel Analysis of Surface Waves, MASW, elastic moduli, deformation modulus, experimental investigations, Plate Load Test, PLT, Triaxial Test, numerical models

Abstract. The paper is devoted to the perspective trend of researches on estimation of physical and mechanical characteristics of dispersive soils by means of non-destructive methods of in-situ testing by wave analysis. The paper presents the results of comparison of the values of the transition coefficient between the soil dynamic elastic modulus, which can be calculated from the results of in-situ tests by means of non-destructive technique of Multichannel Analysis of Surface Waves, and the soil deformation modulus. Application of such a transition factor makes it possible to estimate the soil deformation modulus according to the soil elastic characteristics determined using modern non-destructive express techniques of wave analysis of the low velocity zone of the upper part of the profile. Due to the application of such express methods, labor and time costs of field investigations are significantly reduced during preliminary geotechnical site assessment. Comparison of different values of the transition factor was made on the basis of the results of laboratory standard triaxial tests and numerical experiments with the values calculated on the basis of dependencies proposed by the results of in-situ tests with Plate Load Tests and Multichannel Analysis of Surface Waves in previous in-situ studies. The results of standard triaxial tests on samples of cohesive and non-cohesive soils confirm the dependence of the transition factor on the soil unit weight, obtained in the previous stage of in-situ researches. The values of the transition factor based on the results of numerical experiments do not exceed the results obtained by field research methods. The results of the research will be useful in estimating the physical and mechanical properties of the soil during preliminary geotechnical calculations of the foundations. All in-situ investigations are carried out using non-destructive technique. No permits or approvals are required to perform the work according to the proposed methodology.

1. Introduction

At present, obtaining initial data about soils strata and also physical and mechanical characteristics for geotechnical calculations can take quite a long time, and application of conventional test methods requires relatively large labor costs at the preparation and execution stages. These disadvantages are clearly apparent when conducting an express preliminary geotechnical assessment of the soil base of a future or existing building or structure. The task of reducing the labor and time required to conduct a preliminary geotechnical situation assessment at the pre-design stage is relevant. To solve this problem, modern non-destructive wave methods can be used, in particular, Multichannel Analysis of Surface Waves (MASW).

MASW is a modern non-destructive technique of wave analysis of the low velocity zone at the upper part of soil profile, which allows obtaining a velocity profile of the surface wave distribution in the upper section. MASW was first presented in the Park et al paper. [1]. Different researchers (C.B. Park, J. Xia, S. Foti, J.N. Louie, N. Ryden, K. Suto, R. Miller, M. Carnevalle, Z. Lu, B. Mi, A. Levshin, C. Li et al. [2–14]) continue to improve the technique, increasing the speed of the in-situ procedure and the resolution of velocity profiles. The results of MASW are generally used for dynamic (elastic) soil calculations [15–19], but they can also be used for preliminary geotechnical assessment of soil bases. In the Russian Federation, the Regulation SP 11-105-97 "Engineering geological site investigations for construction. Part VI. Regulations for geophysical surveys" presents several empirical dependencies to determine the deformation modulus (calculated by service limit state) as well as cohesion and the internal friction angle (calculated by ultimate limit state) based

on longitudinal and/or transverse wave velocities for different types of dispersed soils. No such dependencies are given for the surface wave velocity that can be determined using MASW.

Conventional Plate Load Tests (PLT) are used in the Russian Federation to determine the deformation modulus of the soil base during engineering and geological surveys. Deformation modulus corresponds to the straight-line section of the load-settlement curve of PLT in accordance with the State Standard GOST 20276-2012 "Soils. Field methods for determining the strength and strain characteristics". The straight-line section ends at the fourth point of the load-settlement chart, counting from the point of accepted initial pressure. In previous papers of the authors [20, 21], based on comparison of the in-situ PLT and MASW tests, the dependence (1) was proposed to estimate the deformation modulus *E* using the initial shear modulus G_0 and transition factor k_G. Non-dimensional transition factor k_G can be calculated by means of empirical relation (2) as a function of the soil unit weight.

$$E = k_G G_0 \tag{1}$$

$$k_G = -0.005286\gamma^3 + 0.314254\gamma^2 - 6.248539\gamma + 41.723895 \tag{2}$$

where E is deformation modulus, corresponding to the PLT deformation modulus E_{PLT} for a 5000 cm^2 round plate, MPa; G_0 is the initial shear modulus, MPa, it can be estimated using (3) [22] via density (unit weight) and surface wave velocity based on MASW results [20, 21]; γ is the soil unit weight, kN/m^3, it can be estimated using (4) [22] via surface wave velocity, proposed on the basis of known empirical relationships for shear wave velocity [23, 24].

$$G_0 = 1.096 \cdot 10^{-6} \rho V_R^2, \text{MPa} \tag{3}$$

$$\gamma = \ln\left(\frac{V_R^{3.61}}{z^{0.7}}\right) + 0.166372, \text{kN/m}^3 \tag{4}$$

where ρ is soil density, kg/m^3, calculated via soil unit weight; V_R is surface wave velocity, m/s; *z* is soil base depth, m.

To increase the accuracy of dependence (2) inferred from in-situ tests it is necessary to compare it with the results of deformation modulus determination on the basis of triaxial tests, because of all laboratory tests only triaxial tests simulate the behavior of soil under load most closely to the actual behavior [25]. In addition, it is also necessary to carry out numerical experiments based on the results of triaxial tests, since the numerical modeling at preliminary geotechnical assessment of soil bases allows us to eliminate the need for costly and lengthy field tests and, at the same time, to calculate the parameters required for engineering calculations.

The purpose of the paper is to compare the values of transition factor between the elastic modulus and the deformation modulus obtained by means of field tests [20, 21], laboratory triaxial tests and numerical experiments.

2. Methods

2.1. Triaxial tests

Comparison of the values of transition factor between the elastic and deformation moduli was performed based on the results of standard drained triaxial tests of cohesive and non-cohesive soil samples with predescribed parameters at a full water-saturated state (Table 1, soils a and b). The tests were carried out with a triaxial compression unit GT 2.0.9 manufactured by NPP Geotek, LLC (Penza City, Russian Federation), and pressure control panel GT 2.0.11 with static and kinematic loading modes, maximum load of 1 ton (10 kN). Tests were performed in the triaxial compression cell GT 2.3.8 of type A (isotropic compression), the test data was processed using the ASIS automatic software.

To reduce the amount and time of triaxial tests, an analysis of the provided results of triaxial tests on the samples of cohesive soils was performed. The results were provided by NPP Geotek, LLC and the "MIKS" Center for Technological Innovation and Modernization in Construction at PNRPU (Table 1, soils c – g).

The summary list of soils studied in laboratory conditions:

a is fine, saturated, dense sand;

b is heavy, tough clay;

c is medium-hard, light, silt clay;

d is very soft sandy clay;

e is very soft sandy clay;

f is soft, silt clayey sand.

Table 1. Physical parameters of the studied soils.

Soil	z^* (m)	W	W_L	W_P	I_P	I_L	ρ (g/cm³)	ρ_s (g/cm³)	ρ_d (g/cm³)	e	S_r
a	1.5	0.22	–	–	–	–	2.01	2.66	1.68	0.58	1.00
b	1.5	0.24	0.39	0.11	0.28	0.47	1.85	2.74	1.65	0.66	1.00
c	6.5	0.25	0.40	0.22	0.18	0.15	1.98	2.73	1.59	0.72	0.94
d	2.5	0.22	0.27	0.11	0.16	0.69	1.79	2.54	1.47	0.73	0.77
e	4.5	0.23	0.27	0.12	0.15	0.73	1.85	2.54	1.50	0.69	0.84
f	3.9	0.24	0.26	0.23	0.03	0.33	1.97	2.58	1.59	0.62	0.99

z^* is sampling depth, for soils a and b the depth is specified; W is water content; W_L is liquid limit; W_P is plastic limit; I_P is plasticity index; I_L is liquidity index; ρ is density; ρ_s is particle density; ρ_d is dry soil density; e is void ratio; S_r is degree of saturation.

The samples with prescribed parameters were formed according to State Standard GOST 30416-2012 “Soils. Laboratory testing. General”. Before installation on the cell base the samples of sandy soil were previously stabilized at a negative temperature for 1 hour. The formed sample was squeezed out of the holder using a special device and installed in the triaxial cell.

To restore the assumed natural state of the studied soils, the reconsolidation of the prepared samples was carried out by the phase state restoration method (a special case of the backpressure method) in automatic mode, according to Appendix E of State Standard GOST 12248-2010 “Soils. Laboratory methods for determining the strength and strain characteristics”.

Cell pressure increment and stabilization period were assigned according to Table 5.4 of State Standard GOST 12248-2010 (Table 2). Due to the fact that in-situ tests were conducted at a shallow depth in the low-velocity zone, a "sensitive" model at low cell pressures was adopted for triaxial tests.

Table 2. Parameters of triaxial tests.

Parameters	a	b
Vertical overburden pressure σ_1 (kPa)	30	30
Cell pressure σ_3 (kPa)	30	30
Cell pressure increment (kPa)	30	30
Stabilization period of PSR method (min)	5	30
Stabilization period (h)	0.5	18
Loading/unloading rate (mm/min)	0.001	
Unloading stages by deformation value (%)	0.05; 0.10; 0.15; 0.20; 0.30; 0.40; 0.50; 1.00; 2.00; 3.00; 4.00; 5.00	
Sample sizes, $h \times d$ (mm × mm)	100×50	

The deformation curve obtained as a result of triaxial tests was used to determine the soil deformation modulus E. The deformation modulus is not a constant value. Its values depend on the loading interval [25] determined by the future load on the soil from the foundation. At a preliminary estimation of the deformation modulus, the future loads are not yet known, therefore, like the assumption about the first four points of the load-settlement curve in State Standard GOST 20276-2012, deformation modulus was determined for the initial linear section of the deformation curve directly from the charts. The first point of the deformation modulus interval corresponds to overburden pressure in accordance with State Standard GOST 20276-2012, so when defining the deformation modulus from deformation curves, the initial point was taken as zero deviatoric load $\sigma_{\text{dev}} = 0$. The end point of linear approximation by the deformation modulus is taken for relative deformation $\varepsilon_1 = 0.005$. The deformation modulus was calculated according to formula (5).

$$E = \frac{\sigma_{\text{dev}}}{\varepsilon_1} \tag{5}$$

For further calculation of the transition coefficient, the static elastic modulus $E_{0,\text{st}}$ was also determined. For this, an unloading-reloading of the samples was carried out at different relative deformations (Table 2) to determine the values of recovering strains at specific pressure, and the unloading modulus was taken equal

to the static elastic modulus, similar to [26], at a relative strain of the order 10^{-3} (restored strain being not more than 10^{-4}).Then the dynamic elastic modulus $E_{0,\text{dyn}}$ was estimated based on the value of static elastic modulus using coefficient K which is the ratio of dynamic and static moduli of elasticity according to (6) and Fig. 1 proposed in [26]. The dynamic modulus of elasticity was taken for deformations of less than 10^{-6}, which occur during the field tests by MASW method.

$$K = \frac{E_{0,\text{dyn}}}{E_{0,\text{st}}} \tag{6}$$

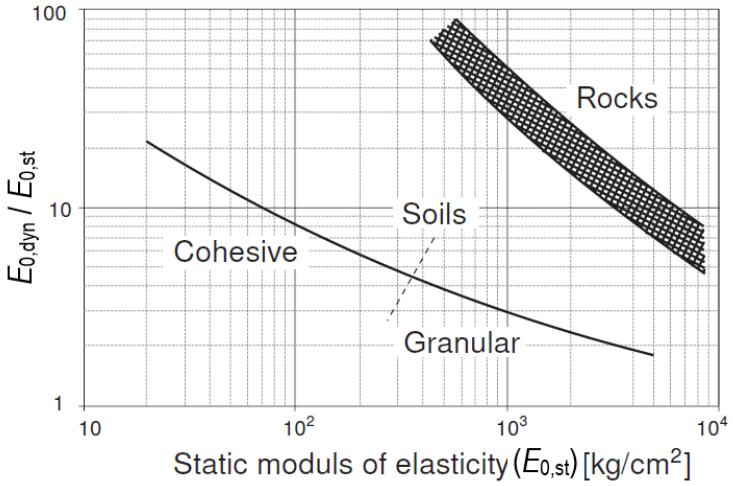

Figure 1. Empirical curve of dynamic and static elastic moduli ratio proposed in [26].

To shorten the test time, the kinematic loading mode was adopted. To create a "sensitive" model, the smallest loading rate of 0.001 mm / min possible for the device was taken (Table 2). Tests were carried out until the destruction of the sample or up to the maximum relative deformation of the sample of 0.15 according to paragraph 5.3.6.13 of State Standard GOST 12248-2010.

Provided results of triaxial tests on cohesive soils (Table 1, soils c–g) did not contain unloading stages, so it was not possible to determine the static modulus of elasticity directly, and the dynamic elastic modulus could not be estimated from Fig. 1 either. Therefore, the dynamic modulus of elasticity was estimated indirectly. First, the surface wave velocity V_R was estimated using formula (4). Further, the initial shear modulus G_0 was calculated from the theory of elasticity using a well-known formula (3). Finally, the dynamic elastic modulus $E_{0,\text{dyn}}$ was estimated via formula (7) using dynamic Poisson's ratio.

$$E_{0,\text{dyn}} = 2G_0\left(1+\nu_{\text{dyn}}\right), \text{MPa} \tag{7}$$

where G_0 is the initial shear modulus, MPa; ν_{dyn} is the dynamic Poisson's ratio assumed by Appendix G of Regulations SP 23.13330.2018 "Foundations of hydraulic structures".

2.2. Numerical modeling

Numerical modeling to determine transition factor values was carried out by modeling in-situ PLT tests by a plate of 5000 cm^2 (diameter $D \approx 80$ cm) in the conditions of natural soil occurrence at the depth of sampling. It was performed in the PLAXIS 2D software package. The geometric model is axisymmetric, 3.0×3.0 m, boundary conditions are standard. The finite element mesh is very fine. Two vertical distributed loads were applied to the geometrical model: the first was the overburden pressure; the second was a variable step load applied to the plate. Loading was made by stages accepted in accordance with State Standard GOST 20276-2012 depending on the soil type and void ratio.

Numerical experiment was carried out using the model of Hardening Soil [27] with Small Strains (HSSS) [28, 29]. The initial shear modulus G_0 was estimated using formula (7) through the dynamic elastic modulus $E_{0,\text{dyn}}$, which in turn was calculated using formula (6) through the ratio K of the dynamic and static moduli of elasticity. The ratio K was estimated using the empirical chart in Fig. 1 [26]. The unloading/loading modulus E_{ur} was assumed to be equal to the static elastic modulus $E_{0,\text{st}}$, which in turn was taken for abraded soils according to the results of triaxial tests, and for intact soils was $E_{0,\text{st}}$ = 6–7 E_{50} (E_{50} was taken from triaxial tests) according to recommendations [30]. The power coefficient *m* of HSSS model [29] was adopted according to recommendations [29] and [31], depending on the soil type. According to [31], the coefficient *m*

is usually assumed to be 0.5 for sand; 1.0 for clay; and intermediate values are assumed for sandy clay and loam.

To improve the accuracy of soil behavior modeling, the parameters of model deformation curves were calibrated in the PLAXIS software module SoilTest on the parameters of triaxial test curves according to the method proposed in [32]. The calibrated soil model parameters are presented in Table 3.

Table 3. Parameters of numerical soil models.

Parameter	a	b	c	d	e	f
Soil model	HSSS	HSSS	HSSS	HSSS	HSSS	HSSS
Material type	Drained	Drained	Drained	Drained	Drained	Drained
γ_{unsat} (kN/m^3)	20.075	20.069	19.404	17.542	18.130	19.306
γ_{sat} (kN/m^3)	20.075	20.069	19.653	18.534	18.713	19.342
e	0.58	0.66	0.72	0.73	0.69	0.62
E_{50}^{ref} (kN/m^2)	14000	10000	7100	4300	7000	8800
E_{oed}^{ref} (kN/m^2)	14000	26400	7100	4300	4000	8800
E_{ur}^{ref} (kN/m^2)	160000	60000	49700	25800	24000	61600
m	0.5	0.9	0.9	0.8	0.8	0.6
c (kN/m^2)	12	13.5	83	10	39	30
φ	41	7	22	19	21	23
ψ	0	0	0	0	0	0
G_0 (kN/m^2)	140000	170000	66400	45000	43000	77000
$\gamma_{0.7}$	2.00E-04	1.00E-05	1.00E-05	8.84E-05	3.51E-04	1.47E-04
p^{ref} (kN/m^2)	30	30	150	100	100	77
R_f	0.9	0.9	0.9	0.9	0.9	0.9

γ_{unsat} is soil unit weight; γ_{sat} is saturated soil unit weight; e is void ratio; E_{50}^{ref} is the secant deformation modulus at 50 % of the maximum deviatoric stress; E_{oed}^{ref} is tangent modulus for primary oedometer loading; E_{ur}^{ref} is unloading/reloading modulus; m is power coefficient; c is cohesion; φ is angle of internal friction; ψ is angle of dilatancy; G_0 is initial shear modulus; $\gamma_{0.7}$ is shear strain level at which shear modulus is reduced to about 70 % of G_0; p^{ref} is reference pressure; R_f is failure ratio [23].

The deformation modulus E was calculated according to State Standard GOST 20276-2012 using formula (8) from load-settlement curves obtained during numerical experiments.

$$E = \left(1 - v^2\right) K_p K_1 D \frac{\Delta P}{\Delta S} \tag{8}$$

where v is Poisson's ratio; K_p is the specific-conditions-of-use factor according to paragraph 5.5.2 of State Standard GOST 20276-2012; K_1 is the coefficient that depends on the plate shape, for a round plate K_p = 0.79; D is the plate diameter, cm; ΔP is pressure increment $P_n - P_0$, MPa, P_n is the end of the chosen load interval, P_0 is the initial point of the chosen load interval, according to State Standard GOST 20276-2012, P_0 is usually taken equal to the overburden pressure; ΔS is settlement increment that corresponds to ΔP, cm.

2.3. Transition factor k_E

After determining deformation and elasticity moduli, the transition factor was calculated. For ease of comparison, instead of the transition factor k_G, the transition factor k_E (9) between the dynamic elastic modulus $E_{0,dyn}$ and the deformation modulus E was calculated in the same way [26]. Dynamic elastic modulus can be calculated using the well-known formula (7). The relationship between transition factors k_G and k_E is represented by the formula (10).

$$E = k_E E_{0,dyn} \tag{9}$$

$$k_E = k_G \frac{1}{2\left(1 + v_{dyn}\right)} \tag{10}$$

where ν_{dyn} is dynamic Poisson's ratio that can be evaluated by means of wave analysis or estimated using Appendix G of Regulations SP 23.13330.2018.

3. Results and Discussion

Deformation curves obtained from triaxial tests are shown in Fig. 2. Elastic parameters of soils determined and evaluated during standard drained triaxial tests are presented in Table 4. Accepted loading intervals for the calculation of deformation modulus and its values, as well as obtained values of the transition factor k_E are given in Table 5.

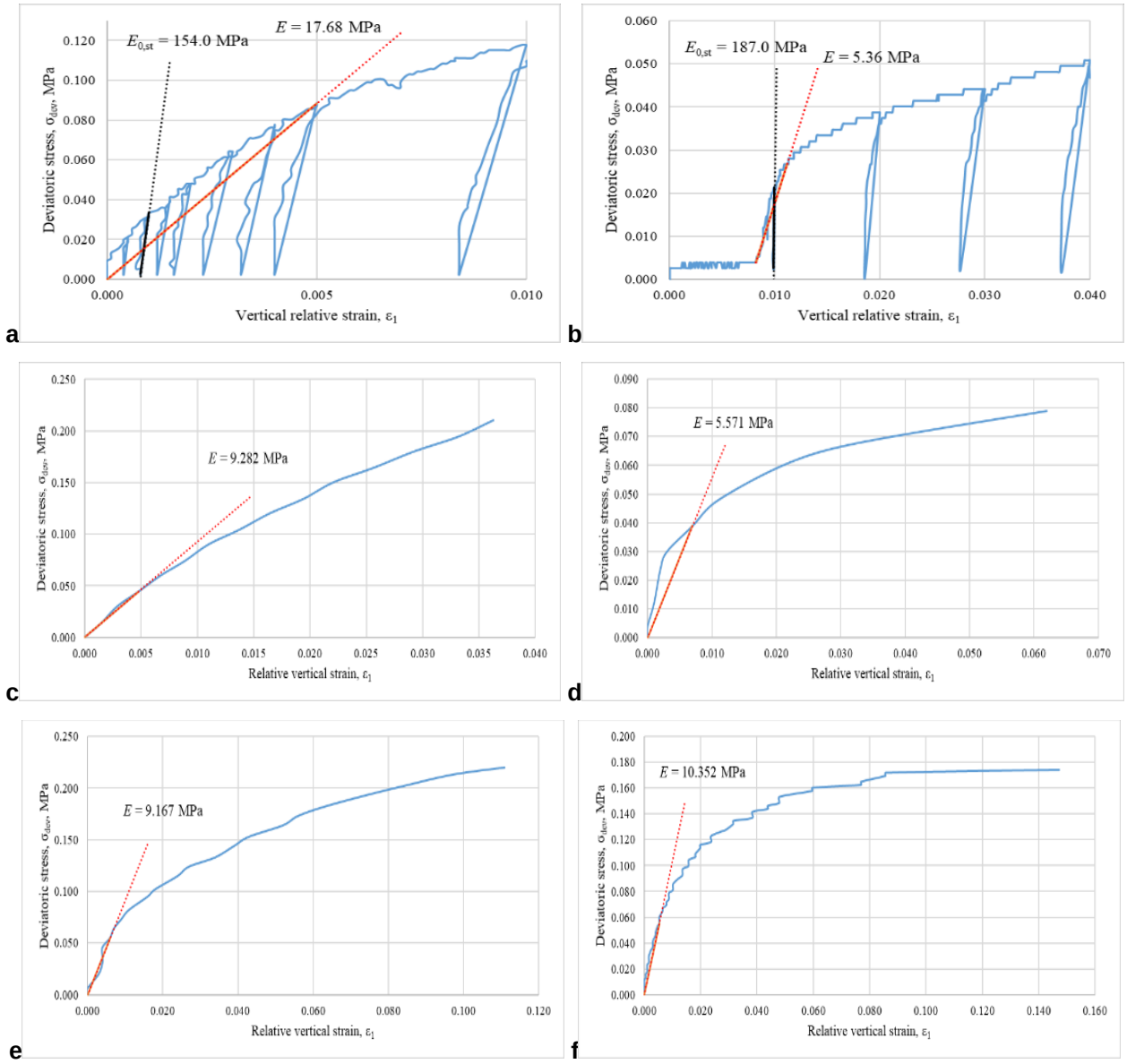

Figure 2. Deformation curves obtained by means of standard drained triaxial tests, the figure letters correspond to soil type letters.

Table 4. Estimation of elastic parameters based on triaxial tests.

Soil	σ_{ov} (MPa)	γ (kN/m^3)	$E_{0,st}$ (MPa)	K	$E_{0,dyn}$ (MPa)	ν_{dyn}	G_0 (MPa)
a	0.030	20.075	154.000	2.5	385.000	0.48	130.068
b	0.030	20.069	187.000	2.5	467.500	0.45	161.207
c	0.150	19.404	–	–	550.915	0.46	188.669
d	0.045	17.542	–	–	121.083	0.44	42.043
e	0.082	18.130	–	–	217.542	0.44	75.535
f	0.077	19.306	–	–	423.139	0.45	145.910

σ_{ov} is overburden pressure; γ is soil unit weight; $E_{0,st}$ is static elastic modulus; K is ratio of dynamic and static elastic moduli according to (6) [26]; $E_{0,dyn}$ is dynamic elastic modulus; ν_{dyn} is dynamic Poisson's ratio estimated using Appendix G of Regulations SP 23.13330.2018; G_0 is initial shear modulus.

Table 5. Estimation of elastic parameters based on triaxial tests data k_E from triaxial tests.

Soil	σ (MPa)	ε_1	E (MPa)	$E_{0,dyn}$ (MPa)	k_E triaxial
a	0.0884	0.0050	17.680	385.000	0.046
b	0.0268	0.0050	5.360	467.500	0.011
c	0.0439	0.0047	9.282	550.915	0.017
d	0.0279	0.0050	5.571	121.083	0.046
e	0.0550	0.0060	9.167	217.542	0.042
f	0.0557	0.0054	10.352	423.139	0.024

σ is deviatoric stress; ε_1 is axial strain, corresponding to the deviatoric stress σ.

The total calculation of the deformation modulus from numerical experiments is shown in Table 6. It was assumed that the tests were performed in the borehole, so, according to State Standard GOST 20276-2012, the K_p coefficient is assumed to be 1.0. Calculation of transition factor k_E values based on the results of numerical experiments is presented in Table 7. Final comparison of obtained transition coefficient k_E values based on the triaxial tests and numerical experiments with the values according to proposed formulas (1) and (2) on the results of PLT and MASW is presented in Table 8 and Fig. 3.

Table 6. Calculation of deformation modulus E from numerical experiments.

Soil	h_{PLT} (m)	ν	P_1 (MPa)	P_4 (MPa)	S_1 (cm)	S_4 (cm)	E (MPa)
a	1.5	0.30	0.030	0.180	0.18	0.67	17.61
b	1.5	0.42	0.030	0.060	0.29	0.37	18.37
c	6.5	0.42	0.150	0.300	5.80	6.66	9.11
d	2.5	0.35	0.045	0.120	1.08	1.78	5.98
e	4.5	0.35	0.082	0.157	4.15	4.94	5.31
f	3.9	0.30	0.077	0.227	2.23	3.09	9.98

h_{PLT} is plate depth; ν is Poisson's ratio; K_p is specific-conditions-of-use factor; P_1 and P_4 are first and fourth points of load-settlement curves; S_1 and S_4 are settlements at P_1 and P_4 respectively; E is deformation modulus.

Table 7. Evaluation of transition factor k_E from numerical tests.

Soil	G_0 (MPa)	ν_{dyn}	$E_{0,dyn}$ (MPa)	E (MPa)	k_E numerical
a	140.000	0.48	414.400	17.606	0.042
b	170.000	0.45	493.000	18.371	0.037
c	66.400	0.46	193.888	9.111	0.047
d	33.000	0.44	95.040	5.985	0.063
e	36.300	0.44	104.544	5.305	0.051
f	77.000	0.45	223.300	9.985	0.045

Table 8. Overall comparison of different values of transition factor k_E.

Soil	k_E PLT	k_E triaxial	Deviation of the triaxial k_E from the PLT one (%)	k_E numerical	Deviation of the numerical k_E from the PLT one (%)
a	0.050	0.046	-8.5	0.042	-15.3
b	0.051	0.011	-77.6	0.037	-27.3
c	0.056	0.017	-69.7	0.047	-15.6
d	0.091	0.046	-49.3	0.063	-30.7
e	0.075	0.042	-43.8	0.051	-32.4
f	0.057	0.024	-57.1	0.045	-21.6

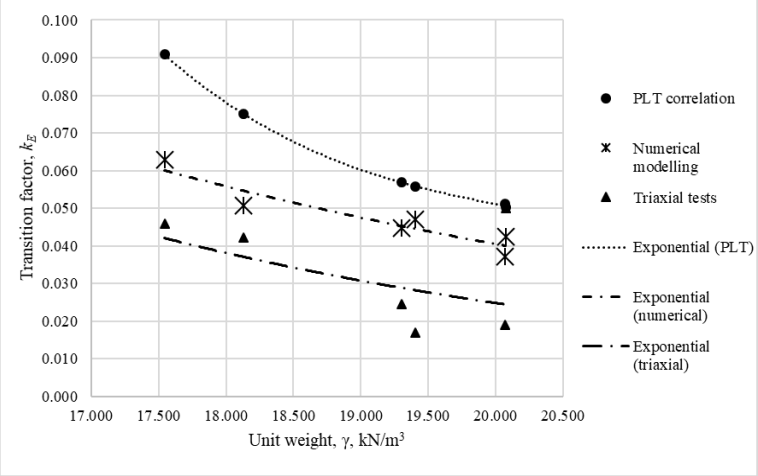

Figure 3. Overall comparison of different values of transition factor k_E.

The comparison of different values of the transition factor confirms its dependence on the soil unit weight.

The lowest values of the transition factor k_E (and, accordingly, the deformation modulus E) were obtained for the triaxial tests, and the highest values were obtained for formula (10) on the basis of the dependencies derived from in-situ tests with PLT and MASW. The deviation of the triaxial test results from the in-situ dependencies does not exceed 78 %.

The results of numerical simulation do not exceed the calculated in-situ dependencies, and the deviation of numerical values from the calculated in-situ ones does not exceed 33 % to the lesser side.

A comparison with the results of experiments performed by other researchers is not given in the article because the transition factor between the elastic modulus and the deformation modulus are determined by the results of MASW for the first time.

4. Conclusions

1. Standard drained triaxial tests allow evaluating dynamic and static modulus of elasticity during a single experiment.

2. The triaxial tests on cohesive and non-cohesive soil samples confirm the dependence of the transition factor on the soil unit weight.

3. The deviation of triaxial test results from in-situ dependencies is not more than 78 %.

4. The comparison of the transition factor k_E from the dynamic modulus of elasticity to the deformation modulus based on the results of in-situ tests and numerical experiments showed that the deviation of the numerical experiments results is not more than 33 % to the lesser side. Values of the transition factor k_E by the results of numerical experiments are less than values of this factor by the results of in-situ tests. This indicates sufficient accuracy of the proposed dependencies (1) and (2) for express assessment of the soil deformation modulus based on the wave analysis by MASW at a preliminary geotechnical site assessment.

5. Correctness of numerical modeling depends on the adequacy of adopted soil model, which requires calibration of input parameters and, accordingly, of the model deformation curve on the experimental deformation curve based on standard triaxial tests.

5. Acknowledgements

The authors thank the research support services of Perm National Research Polytechnic University for providing the equipment for field and laboratory testing. This research did not receive any specific grant funding from agencies in the public, commercial, or not-for-profit sectors.

References

1. Park, C.B., Miller, R.D., Xia, J. Multichannel analysis of surface waves. Geophysics. 1999. 64(3). Pp. 800–808. DOI: 10.1190/1.1444590
2. Xia, J., Miller, R., Park, C.B. Estimation of near-surface shear-wave velocity by inversion of Rayleigh waves. Geophysics. 1999. No. 64. Pp. 691–700. DOI: 10.1190/1.1444578
3. Foti, S. Multistation methods for geotechnical characterization using surface waves. PhD thesis. [Online]. System requirements: AdobeAcrobatReader. URL: http://www.soilmech.polito.it/content/download/117/592/file/SF_Phd_diss.pdf (date of application: 01.02.2020).
4. Louie, J.N. Faster, Better: Shear-Wave Velocity to 100 Meters Depth from Refraction Microtremor Arrays. Bulletin of the Seismological Society of America. 2001. 91(2). Pp. 347–364. DOI: 10.1785/0120000098

5. Ryden, N., Park, C.B. Fast simulated annealing inversion of surface waves on pavement using phase-velocity spectra. Geophysics. 2006. 71(4). Pp. R49–R58. DOI: 10.1190/1.2204964
6. Suto, K. Multichannel analysis of surface waves (MASW) for investigation of ground competence: an introduction. Proceedings of the Sydney Chapter 2007 Symposium. Australian Geomechanics Society. Sydney, 2007. Pp. 71–81.
7. Park, C.B., Miller, R.D. Roadside Passive Multichannel Analysis of Surface Waves (MASW). Journal of Environmental and Engineering Geophysics. 2008. 13(1). Pp. 1–11. DOI: 10.2113/JEEG13.1.1
8. Park, C.B., Carnevale, M. Optimum MASW survey – revisit after a decade of use. Proceedings of GeoFlorida 2010, Advances in Analysis, Modeling, and Design, Florida, Feb. 20-24, 2010. American Society of Civil Engineering. West Palm Beach, 2010. Pp. 1303–1312. DOI: 10.1061/41095(365)130
9. Lu, Z., Wilson, G.V. Imaging a soil fragipan using a high-frequency multi-channel analysis of surface wave method. Journal of Applied Geophysics. 2017. No. 143. Pp. 1–8. DOI: 10.1016/J.JAPPGEO.2017.05.011
10. Mi, B., Xia, J., Shen, C., Wang, L., Hu, Y., Cheng, F. Horizontal Resolution of Multichannel Analysis of Surface Waves. Geophysics. 2017. 82(3). Pp. EN51–EN66. DOI: 10.1190/geo2016-0202.1
11. Mi, B., Xia, J., Bradford, J., Shen, C. Estimating Near-Surface Shear-Wave-Velocity Structures Via Multichannel Analysis of Rayleigh and Love Waves: An Experiment at the Boise Hydrogeophysical Research Site. Surveys in Geophysics. 2020. Pp. 1–19. DOI: 10.1007/s10712-019-09582-4.
12. Jaganathan, A. Multichannel surface wave analysis of reinforced concrete pipe segments using longitudinal and circumferential waves induced by a point impact. Journal of Applied Geophysics. 2019. No. 163. Pp. 40–54. DOI: 10.1016/j.jappgeo.2019.02.010
13. Sastry, R.G., Chahar, S. Geoelectric versus MASW for geotechnical studies. Journal of Earth System Science. 2019. No. 128. Pp. 13. DOI: 10.1007/s12040-018-1061-x
14. Baglari, D., Dey, A., Taipodia, J. A state-of-the-art review of passive MASW survey for subsurface profiling. Innovative Infrastructure Solutions. 2018. No. 3. Pp. 1–13. DOI: 10.1007/s41062-018-0171-2
15. Levshin, A., Barmin, M.P., Ritzwoller, M.H. Tutorial review of seismic surface waves' phenomenology. Journal of Seismology. 2018. 22(2). Pp. 519–537. DOI: 10.1007/s10950-017-9716-7
16. Li, C., Ashlock, J.C., Lin, S., Vennapusa, P.K.R. In Situ Modulus Reduction Characteristics of Stabilized Pavement Foundations by Multichannel Analysis of Surface Waves and Falling Weight Deflectometer. Construction and Building Materials. 2018. 188(10). Pp. 809–819. DOI: 10.1016/j.conbuildmat.2018.08.163
17. Karray, M., Tremblay, S.-P., Hussien, M., Chekired, M. Importance of coherence between geophysical and geotechnical data in dynamic response analysis. E3S Web of Conferences. 2019. No. 92. 6 p. DOI: 10.1051/e3sconf/20199218007
18. Abudeif, A., Fat-Helbary, R., Mohammed, M.A., Alkhashab, H.M., Masoud, M.M. Geotechnical engineering evaluation of soil utilizing 2D multichannel analysis of surface waves (MASW) technique in New Akhmim city, Sohag, Upper Egypt. Journal of African Earth Sciences. 2019. No. 157. 10 p. DOI: 10.1016/j.jafrearsci.2019.05.020
19. Robertson, P.K. Interpretation of cone penetration tests – a unified approach. Canadian Geotechnical Journal. 2009. 46(11). Pp. 1337–1355. DOI: 10.1139/T09-065
20. Antipov, V.V., Ofrikhter, V.G. Correlation between wave analysis data and data of plate load tests in various soils. Proceedings of the International Conference on Geotechnics Fundamentals and Applications in Construction: New Materials, Structures, Technologies and Calculations, GFAC, Feb. 6-8, 2019. Taylor & Francis Group. London, 2019. Pp. 16–20. DOI: 10.1201/9780429058882-4
21. Antipov, V.V., Ofrikhter, V.G. Field Estimation of Deformation Modulus of the Soils by Multichannel Analysis of Surface Waves. Data in Brief. 2019. 24. 5 p. DOI: 10.1016/j.dib.2019.103974
22. Ofrikhter, V.G., Antipov, V.V. Sposob o͡tsenki modulia͡ deformat͡sii grunta [The method of estimation of soil deformation modulus]. Patent Russia no. 2704074, 2019. (rus)
23. Mayne, P.W. Stress-strain-strength-flow parameters from enhanced in-situ tests. Proceedings of the International Conference on In-Situ Measurement of Soil Properties, Bali, May 21-24, 2001. Parahyangan Catholic University. Bali, 2001. Pp. 27–48.
24. Moon, S.W., Ku, T. Empirical estimation of soil unit weight and undrained shear strength from shear wave velocity measurements. Proceedings of the 5th International Conference on Geotechnical and Geophysical Site Characterization, ISC 2016, Gold Coast, Australia, Sep. 5-Sep. 9, 2016. Australian Geomechanics Society. Gold Coast, 2016. Pp. 1247–1252.
25. Boldyrev, G.G., Melnikov, A.V., Novichkov, G.A. Part IV. Interpretation of Laboratory Test Results to Determine Soil Deformation Characteristics. Engineering survey. 2014. No. 5-6. Pp. 98–105. (rus)
26. Alpan, I. The geotechnical properties of soils. Earth Science Reviews. 1970. 6(1). Pp. 5–49. DOI:10.1016/0012-8252(70)90001-2.
27. Duncan, J.M., Chang, C.Y. Nonlinear Analysis of Stress and Strain in Soils. Journal of the Soil Mechanics and Foundation Division. 1970. 96(SM5). Pp. 1629–1653.
28. Hardin, B.O., Drnevich, V.P. Shear modulus and damping in soils: Design equations and curves. Journal of the Soil Mechanics and Foundation Division. 1972. 98(SM7). Pp. 667–692.
29. Brinkgreve, R.B.J. (ed). Plaxis Material Models Manual. [Online] System requirements: AdobeAcrobatReader. URL: https://www.plaxis.com/?plaxis_download=2D-3-Material-Models.pdf (date of application: 11.12.2019).
30. Melnikov, R.V. Oedometer test data for finding Hardening Soil model. Akademicheskij Vestnik UralNIIproekt RAASN. 2014. No. 4. Pp. 90–94. (rus)
31. Gouw, T.L. Common mistakes on the application of Plaxis 2D in analyzing excavation problems. International Journal of Applied Engineering Research. 2014. 9(21). Pp. 8291–8311.
32. Melnikov, R.V., Sagitova, R.H. Calibration of Hardening Soil Model Parametres According to the Results of Laboratory Testing in Program "Soiltest". Akademicheskij Vestnik UralNIIproekt RAASN. 2016. No. 3. Pp. 79–83. (rus)

Contacts:

Vadim Antipov, seekerva@mail.ru

Vadim Ofrikhter, ofrikhter@mail.ru